PROCEEDINGS OF SCIENCE

Silicon detectors for precision track timing

Gregor Kramberger[a,*]

[a] *Jožef Stefan Institute,*
Jamova 39, SI-1000 Ljubljana, Slovenia

E-mail: Gregor.Kramberger@ijs.si

Silicon detectors are the most widely used detector technology for precise tracking and vertex detectors at present experiments in particle physics. The requirements for future particle physics experiments are getting even more demanding, not only in required position resolution ($\sim few\mu$m) and reduced pixel sizes, but also in ability to accurately, on the level of tens ps, measure the time of the particle hitting the detector. Among the hybrid pixel detectors there are two directions of developments. Thin Low gain avalanche detectors exploit internal gain to achieve required S/N and fast signal. On the other hand thicker 3D sensors exploit short drift distance given by vertical electrodes for fast charge collection and adequate signal. Monolithic Active Pixel Detectors offer a compromise between achievable signal/noise and thickness and recent developments exploiting also avalanche multiplication can offer excellent performance. The present paper will discuss basics, strengths and limitations of different technologies and possible directions of future developments.

10th International Workshop on Semiconductor Pixel Detectors for Particles and Imaging (Pixel2022)
12-16 December 2022
Santa Fe, New Mexico, USA

*Speaker

PoS(Pixel2022)010

1. Introduction

Position sensitive silicon detectors are most widely used for tracking of charged particles in most particle physics experiments . They are based on a depleted p-n junction to establish the electric field and low enough free carrier background and offer many advantages over other technologies. Although they are fast with saturated drift velocities of $\sim$ 100 μm/ns and can be made thin and compact they were exploited mainly as position sensitive detectors, hence resolving the charge particle hit position on the scale of several to several tens μm.

The future experiments in the particle physics will often require large collision rates for improved statistics. At High-Luminosity Large Hadron Collider (HL-LHC)[1] there will be on average 140-200 proton-proton collisions per colliding bunches every 25 ns. The track multiplicities will be such that reconstruction of proton collision points using the position information alone would become difficult especially for tracks in forward direction. Reconstructed tracks therefore need to be associated with the time of the collision inside each bunch crossing. That allows better reconstruction and effectively increases integrate luminosity. Required track time resolution is of several tens ps (proton collisions within the colliding bunches are distributed with $\sigma_t \approx 180$ ps and $\sigma_z \approx 5$ cm). Both, ATLAS and CMS experiments plan to use dedicated timing detector using Low Gain Avalanche Detectors (LGAD), HGTD [2] and ETL [3].

Even more demanding requirements will be imposed on tracking detectors at Future Circular Hadron Collider (FCC-hh)[4] foreseen in next decades where a full 4D tracking will be required. A precise time stamp will be associated with the individual tracking sensors hits and not only to the tracks using a dedicated timing detector. This will facilitate much better reconstruction, less CPU power consumption and thus effectively larger effective integrated luminosity.

During the HL-LHC the operation experiments plan to replace the some of their sub-detectors with those being able to provide also timing information, such as VELO detector [5] of the LHCb experiment. CMS and ATLAS consider extracting also timing information from their pixel detectors. Time resolution of several tens ps will be also required for some experiments like NA-62[6] and Klever [7] as well as the beam monitors like for NA-61 [8]. Using these detectors in harsh radiation environments will impose large radiation hardness. The latter will be relaxed in lepton colliders, where superb time (5 ps) and spatial resolutions (few μm) will be also required, but particle rates will be moderate [9].

Apart from the use in particle physics, which remains the key driver of the technology, the use of sensors with superb time resolution will be interesting for medical applications, such as proton-CT[10] and single particle counting beam monitors [11].

2. Timing measurements

The time resolution of any particular sensor can only be considered together with electronics. The two main contributions to the time resolution are time walk and noise jitter (see Fig. 1a).

Time walk is a consequence of variations of induced current shapes for particles hitting the same electrode. That leads to different times of a processed signal crossing the threshold (ToA). The time walk can be mitigated by correcting for different signal heights (e.g. constant fraction discrimination), but due to the stochastic nature of particle energy loss in sensors (ionization

pattern) the time walk cannot be completely removed. The residual time walk is often referred to as contribution due to Landau fluctuations (σ_{lf}). It sets the limits for the time resolution of a given sensor, depending on the velocity profile. In a segmented detector with pitch $\ll$ thickness the induced currents have different shape depending the hit position within the electrode, leading to similar effects as for Landau fluctuations. This contribution to the time walk is often referred to as distortion or weighting field contribution (σ_{wf}).

Different contributions to the time walk are often correlated. The dominant contributions for various electrode configurations are indicated in Fig. 1b. The time walk of the sensor with large electrodes (LGAD with pitch/thickness$\leftarrow \infty$) is dominated by σ_{lf}, a sensor with pitch/thickness < 1 has sizeable σ_{lf} and σ_{wf}. Time resolution of 3D sensors (see next chapter) is dominated by σ_{wf}.

The noise jitter is simply the translation of the electronic noise (N) into the uncertainty in the discriminator crossing time as shown in Fig. 1a. The jitter is minimized by fast signal rise time (dV/dt) and small noise. As the rise time can be approximated by S/t_p (t_p peaking time of electronics, S signal amplitude) the jitter is given by $\sigma_j \approx t_p/(S/N)$. Therefore small electrode capacitance (noise) and short drift time with large signal (induced charge) are crucial.

Finally there are also contributions due to time-to-digital conversion and precision of the reference time. The problem of a timing detector is therefore minimization of the above mentioned contributions with respect to the application.

There are several different technologies investigated to achieve good timing and/or spatial resolution: planar detectors as hybrid sensors exploiting internal sensor gain or monolithic sensors, and 3D sensors where thickness [12] is decoupled from drift path allowing simultaneously short collection time and large signal.

3. Planar sensors

Planar detector suitable for precise timing measurements are of two kinds. Low Gain Avalanche Detectors [13, 14] are similar to conventional $n-p$ diodes (PIN) with an extra layer of highly doped silicon inserted between n and p, thus forming $n^{++}-p^{+}-p$ structure. High doping level of p^{+} layer results in very high electric fields of > 25 V/μm, thus leading to avalanche multiplication. LGADs are connected to electronics as standard planar detectors through bump bonding.

Monolithic pixel detector already include at least first amplification stage in the same wafer, hence offer a possibility of achieving lower noise and better integration/power consumption.

The number of generated e-h pairs and the carrier drift time are proportional to the thickness (d). Signal is proportional to integration time and its maximum is achieved if the entire induced current is integrated. However that requires long peaking times of electronics which adversely affect the jitter.

Assuming saturated drift velocities for electrons ($v_{sat,e,h}$) and holes and peaking time of the amplifier similar to the collection time ($\tau_p \approx d/v_{sat,e} + d/v_{sat,h}$ with gain close to the surface and $\tau_p \approx d/v_{sat,h}$ without gain) the dependence of jitter on sensor thickness can be obtained for different noise levels as shown in Fig. 2a. Most probable signal (S_{MVP}) is given by the ionization density, thickness of the device and possibly gain. It should be noted that at smaller thicknesses most probable charge per unit length becomes smaller [17]. In order to achieve jitter compatible

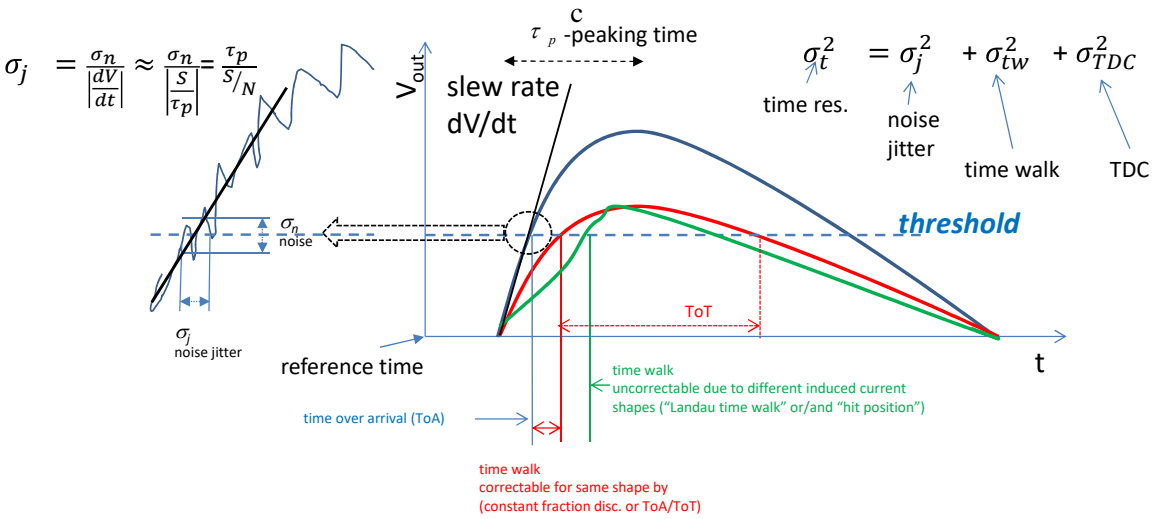

(a)

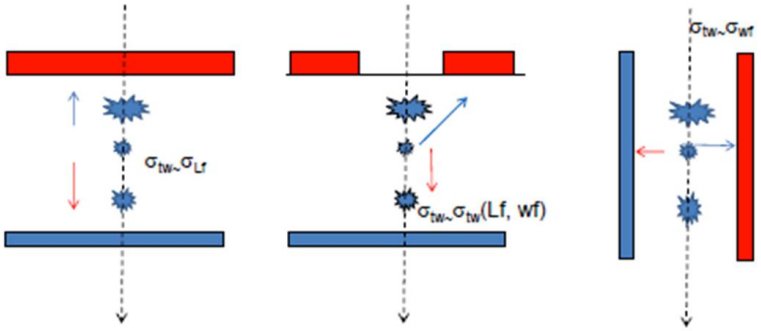

(b)

Figure 1: (a) Contributions to the timing resolution. (b) Examples of the planar pad detector, segmented planar detector and 3D detector detecting the same charged particle. Dominant contributions to the time walk are shown for each of the three cases.

with time resolution of ~ 10 ps, gain becomes a necessity for planar detectors. At equivalent noise charge of ENC = 100 e which is currently the noise level of ATLAS/CMS pixel detector the jitter contribution would be theoretically at the level of 20 ps.

On the other hand arrival of the drifting electrons to the gain layer close to the electrode results in large contribution from σ_{lf} to the time walk as shown in Fig. 2b. The measurements were done for 35, 50 and 80 μm thick LGADs (pad size 1.3×1.3 mm^2) using fast discrete electronics at signals of $S_{MVP} > 20$ fC where the jitter is much smaller than the time walk.

Creation of e-h pairs in LGADs and PINs was simulated for 1 GeV pions in GEANT4. The currents induced by their motion were simulated at most probable signal of 20 fC in LGADs with KDetSim simulation package [18]. A good agreement was found with measurements. Simulation of the σ_{lf} in a PIN detector at the linear field of average 1 V/μm (squares) and in case of saturated velocity (triangle) showed on the other hand much smaller σ_{lf}.

The weighting field contribution should be added approximately in squares to the σ_j and σ_{lf}. It is therefore clear that a single hit time resolution below 10 ps in a segmented detector with a small cell size of order few tens×few tens μm^2 cell size is very difficult to achieve even with a very high gain.

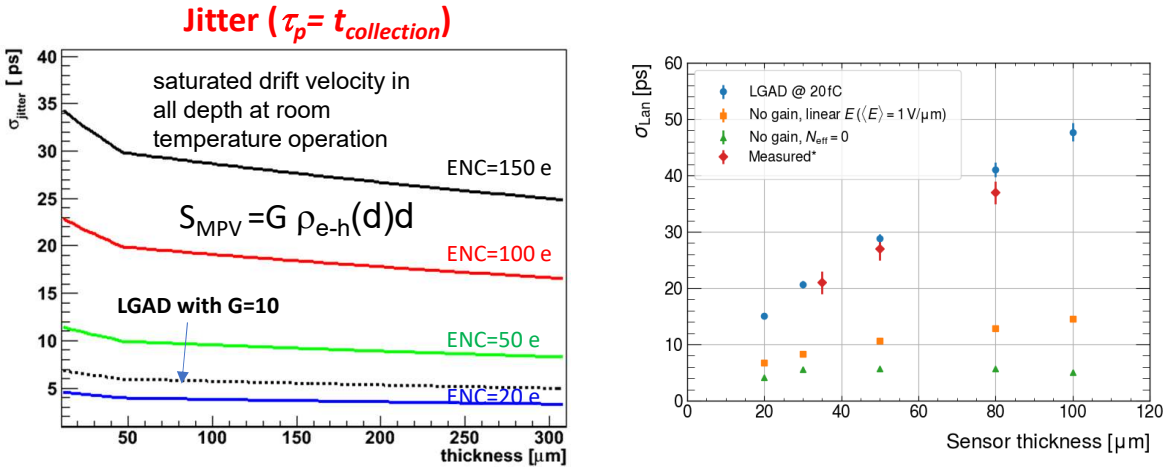

(a) (b)

Figure 2: (a) Dependence of jitter σ_j on device thickness for different levels of electronics noise ENC. An optimal case of saturated drift velocities and electronics peaking time equal to collection time is assumed. b.) σ_{lf} dependence on device thickness for 1 GeV pions (simulation) and measurements for LGADs with ^{90}Sr electrons (data from JSI, UCSC, [2]). Simulated charge in LGADs was 20 fC with saturated drift velocity over the entire depth of the sensor. Constant fraction discrimination at 25% was used to correct for the time walk.

3.1 Hybrid sensors - Low Gain Avalanche Detectors

LGADs offer superb time resolution even for large pad (capacitance) devices, however they have some drawbacks. The main drawbacks of LGAD sensors are their radiation tolerance and active area coverage (fill factor).

A schematic view of the LGAD and the dependence of fill factor on the LGAD design (inter-pad region) is shown in Fig. 3a. The gain layers of two electrodes in a standard LGAD sensor are separated by a gap (x) where there is no gain. The inter-pad region is typically limited to several tens μm ($\sim$ 50μm for ATLAS and CMS) imposed by electrode isolation and prevention of premature breakdown for floating pads. Hence, practical dimensions of pixels are $a \sim 1$ mm.

The radiation tolerance of LGADs has been subject of intense investigation over the last years [19–21]. The main problem is disappearance of active acceptors in the gain layer after hadron irradiations. This so called initial acceptor removal leads to reduction of doping level as deep acceptors are not introduced with enough rate to compensate the removal of the initial ones. In order to compensate the decrease of field the bias voltage must be increased. The LGAD suitable for timing are typically thin $d < 60\mu$m and can be therefore fully depleted up to equivalent fluences of $> 10^{16}$ cm^{-2} [22]. In the first approximation the change of the electric field in the gain layer with irradiation is given by $\Delta E \approx \Delta V_{gl}/x_{gl}$, where gain layer depth is x_{gl} and V_{gl} its depletion voltage.

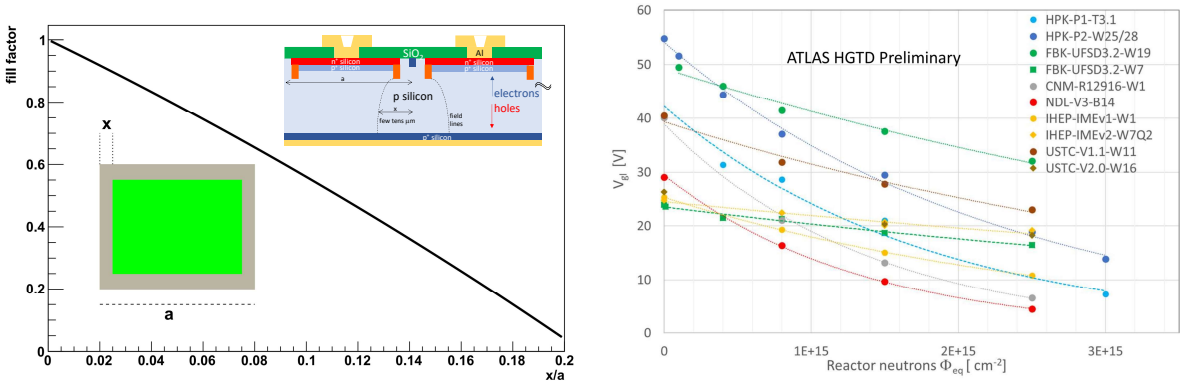

(a) (b)

Figure 3: (a) Active area dependence on the inter-pad distance for an LGAD . The square pixel with side a has the inter-pad distance of $2\,x$. The inset shows a schematic view of a conventional LGAD showing x and bending of field lines (dashed) (b) Evolution of gain layer depletion voltage with fluence for different prototypes as measured by ATLAS collaboration. LGADs with larger larger gain layer depths x_{gl} have typically larger initial V_{gl}. The exponential fits to the measured data are indicated with dashed lines. Note that the smaller slope is for C-enriched devices.

An example of V_{gl} evolution with fluence is shown in Fig. 3b for different detector prototypes of HGTD.

Gain layer depletion voltage decreases exponentially with fluence $V_{gl} = V_{gl,0}\exp(-c\,\Phi_{\rm eq})$, with initial acceptor removal constant c. The large initial V_{gl} corresponds to deep ($x_{gl} \sim 2\mu$m) and smaller to shallow $x_{gl} \sim 1\mu$m. As the required increase of operation voltage to keep the same gain is $\Delta V_{op} \approx \Delta V_{gl} \cdot d/x_{gl}$, several hundreds of volts can be required to compensate for the decrease of V_{gl}. However, the bias voltage can only be raised to the threshold voltage of a single event burnout, $V_{SEB} \approx 12\text{V}/\mu\text{m} \cdot d$ [23, 24]. Above V_{SEB} a high enough energy loss of a single energetic beam particle in a active region can lead to a destructive breakdown of the device.

Different ways of the radiation damage mitigation are investigated, most promising is carbon enrichment of gain layer which decreases acceptor removal constant by almost an order of magnitude (see Fig. 3b)[20]. Other ways of extending radiation hardness include: use of compensated material [25], partial activation of initial boron HAB [26] and high temperature annealing [27]. Currently the radiation hardness of LGADs is limited to fluences of few 10^{15} cm^{-2}.

It is obvious that for small pitch devices (few tens μm) the required inter-pad region is too large (see Fig. 3a) for an efficient detector. There are several ways of avoiding the inefficient inter-pixel gap. Each of them has advantages and drawbacks:

- Inverse-LGAD [28] (Fig. 4a) is based on the idea that non-gain electrodes are segmented. This requires more complex processing (double sided can be avoided nevertheless), but the main concern is that the segmented side collects holes in low electric field. To what extent this degrades the performance after irradiation is yet to be established. However, acceptor removal will require application of high bias voltage, hence electric field and the difference in trapping distances for electrons and holes will be small. Therefore their performance may be comparable with conventional LGADs.

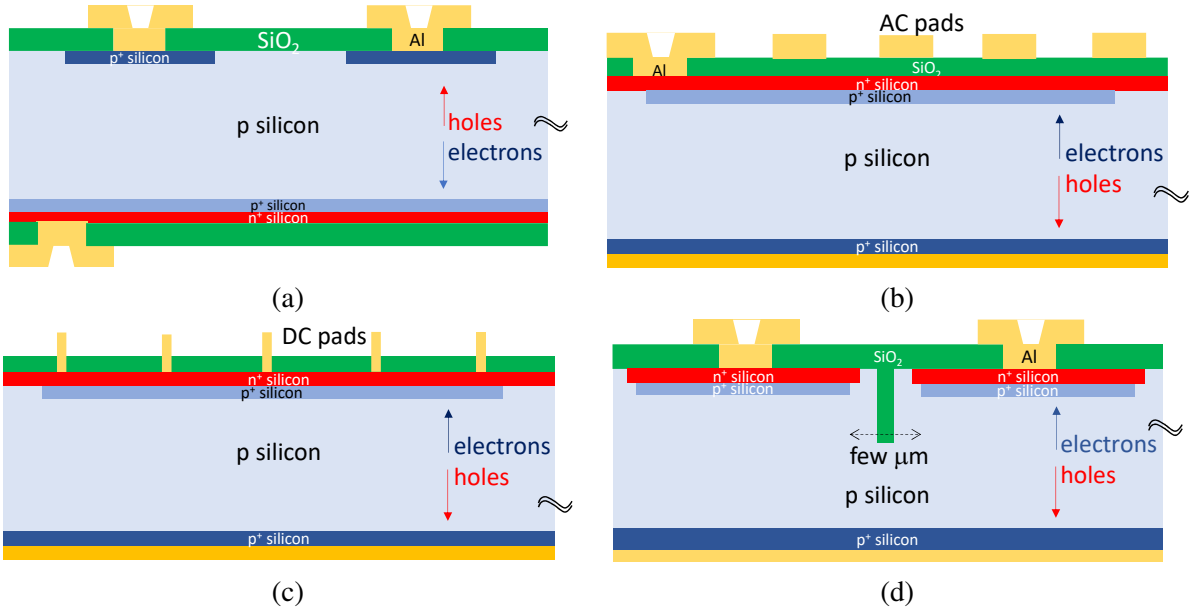

Figure 4: Different types of LGAD sensor offering good fill factor: (a) Inverse-LGAD, (b) AC-LGAD , (c) DC-Resistive-LGAD and (d) Trench Isolated - LGAD.

- AC-LGAD [29] (Fig. 4b) are similar to the AC coupled silicon strip detectors. A n^+ layer acts like a resitive layer slowly discharging the electrons produced in the multiplication. These devices are limited as at high rates the bipolar pulses in sensing electrodes will overlap - shift of the signal base line and there could be also substantial signal induction in neighbouring electrodes. Moreover, radiation may affect also the resistivity of n^+ layer and by that the signal formation.

- DC-RSD LGAD [30] (Fig. 4c) are similar to AC-LGAD, but the coupling oxide is completely removed. The narrow cross-shaped neighboring electrodes restively share charge. Measurements have shown a superb position and time resolution. The use of large readout pitch is beneficial for achieving superb time and position resolution with reduced density of readout nodes. Similarly to AC-LGADs these devices have limited rate capability. The same considerations concerning the radiation damage as for AC-LGADs remain.

- Trench Isolated LGADs [31] (Fig. 4d) are similar to standard LGADs with innovative electrode isolation technique. The isolation is achieved with one or more SiO_2 trenches between the pixels. The electric field lines in the inter-pad region, which is of only few μm, end mainly in the gain layer.The effective inter-pad gap of only few μm was achieved [32] thus allowing small pitch devices.

3.2 Monolithic sensors

Monolithic sensors where electronics and sensors are made on the same wafer are likely to replace conventional strip and pixel detectors as large surface tracking detectors. Their ultimate timing capabilities are limited by being planar, but their better integration and noise performance

can lead to an improvement of performance with respect to the conventional planar hybrid detectors. Present monolithic sensors utilize either small or large collection n^+ electrode design shown in Fig. 5. Neither of both types has a clear preference with respect to the timing applications.

The narrow electrode design has much smaller capacitance (noise), can use thin active zone and by that minimize σ_{lf}, but suffers from large σ_{wf} as there is a large difference in drift time depending on the hit position of the particle (see drift paths in the Figs. 5a,b). At a given cell size a the the drift lengths for a thin active zone d ($a > d$) are roughly given by the $a/2$. Assuming saturated electron drift velocity in the lateral direction, which is very difficult to achieve, the limit is $\sigma_{wf} > \frac{a}{2}$ ps/μm. On the other side wide electrode design is very similar to the conventional planar detectors and is limited to $\sigma_t > 50$ ps.

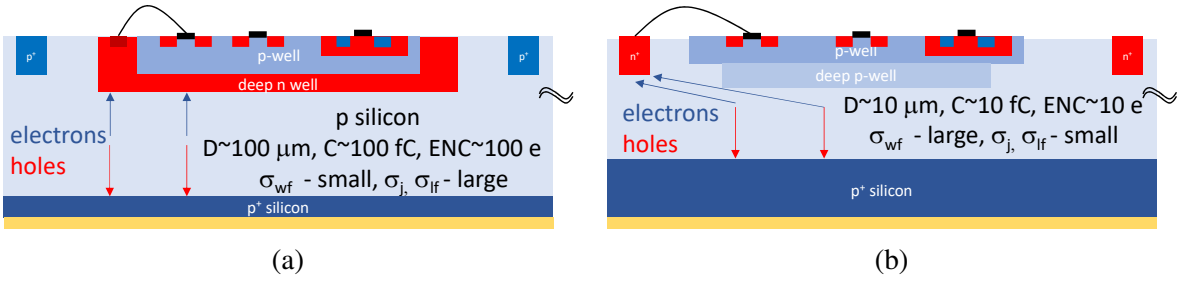

Figure 5: Schematic view of the depleted Monolithic Active Pixel Devices: (a) Large-electrode design (b) Small-electrode design with backside biasing. Typical properties and expected contributions to the time resolution are given. The direction of drift for electrons and holes is also indicated.

A novel approach is a monolithic active pixel detector with gain. In addition to the benefits of the latter, advanced BiCMOS processes with SiGe front-end transistors can be faster than silicon and allow at the same speed lower noise. An example is shown in Fig. 6 where a so called PicoAD detector is shown [33]. A thin active layer (5 μm) is formed at the back followed by a fully depleted gain layer. The multiplied electrons drift across the drift zone of $\sim$ 10μm) to the input node of the amplifier. Although the e-h pairs created in the drift zone also contribute to the signal (may also lead to h multiplication) its main goal is to decouple the gain layer from the electronics layer and mitigate the loss of efficiency in the inter-pixel region. These devices should offer a superb time resolution of 10 ps (first prototypes 20 ps), but are likely to be less radiation hard than conventional LGADs. Thin active zone also means less ionization density wrt e.g. 50 μm thick LGAD and larger fluctuations.

4. 3D sensors

From their proposal 3D detectors were envisaged to offer good timing properties [34], but have only recently been investigated for the ultimate time performance [35–37]. As the drift path is separated from the thickness (signal), fast rise-time and good enough S/N required for small jitter can be achieved without gain. Small distance between electrodes also minimizes σ_{lf}, which unlike in LGADs, contribute to much smaller extent to the time resolution (for approximation use Fig. 2b with electrode distance as thickness). Small inter-electrode distance and by that full depletion voltage ensure high radiation hardness. 3D sensors of small 50×50 μm^2 cells have demonstrated efficient operation up to equivalent fluences of $3 \cdot 10^{16}$ cm^{-2} [39].

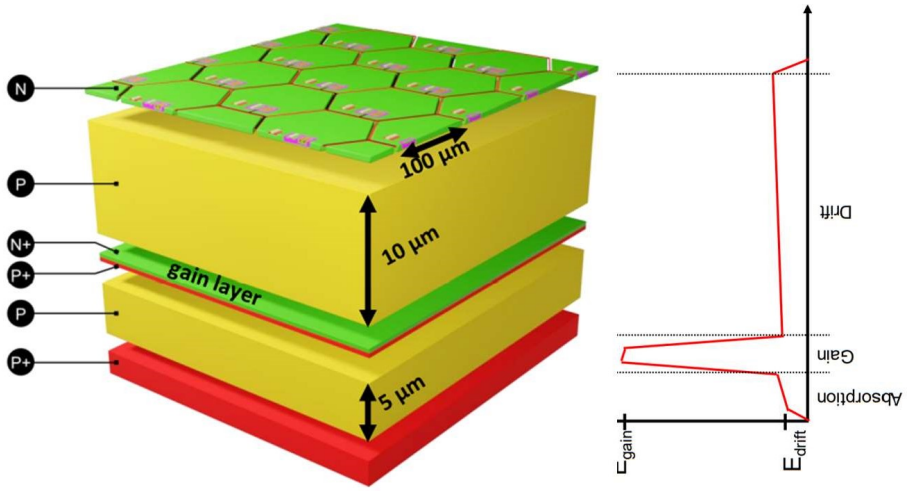

Figure 6: A schematic view of the PicoAdd detector (taken from []) and the electric field profile in the sensor. Please note the figure in not to scale.

There are two main directions in 3D sensor design suitable for timing. A conventional Column-3D sensors, essentially the same as for ATLAS/CMS pixel detectors at HL-LHC with possibly optimized column layout for timing and so called Trench-3D detectors developed within the Time Spot project [37, 38]. They are depicted in the Fig. 7.

Threch-3D devices reache theoretical limit of σ_{wf} for the given cell size. The cell can be seen as two back to back thin pad detectors. Short drift distance (half of the cell dimension, $a/2$) and large thickness ($d >> a/2$), minimize σ_{lf} as well, except for the inter-cell region. A superb time resolution of 20 ps was reached in the test beam using a few cell readout with discrete electronics, also designed in the framework of Time-Spot collaboration. A detailed analysis of the data yielded $\sigma_{wf} < 10$ ps. The achievable time resolution is therefore dominated by the the jitter. Being 3D and thin with almost no low field region make these devices very radiation hard. Almost independent time resolution on the fluence was measured up to $2 \cdot 10^{16}$ cm^{-2}. The major problem for the Trench-3D production is scaleability of production with high yield and complex handling of the wafers.

A conventional Column-3D sensors ($50\times50\,\mu$m^2) have also demonstrated good time resolution up to equivalent fluence of 10^{16} cm^{-2} (see Fig. 8)a [36]. The contributions to the time resolution measured with discrete electronics show σ_{wf} as dominant contribution, which is at the comparable cell size worse than for the Trench-3D. The measured values agree with simulated, where the simulation predicts the time resolution of around 13 ps for $25 \times 25\,\mu$m^2 cell size [35]. The time resolution for a group of several cells connected to the same amplifies leads to further improvement of the resolution for the inclined tracks.

There are several drawbacks of the 3D detectors. The electrode capacitance is much larger than for planar detectors which affects noise (also power consumption) and by that jitter (see Fig. 9a). The column/trench widths impact the capacitance, electric field and fill factor. 3D sensors will therefore profit from improvements of Deep Reactive Ion Etching (DRIE) in the future along with

optimized electrode configuration for timing. 3D sensors are not 100% efficient for perpendicular tracks (see Fig. 9b). While Column-3D are generally fully efficient for inclined tracks, this is not so for Trench-3D which can have inclined direction where the active zone isn't hit.

Possibly the largest obstacle is their thickness which is required for good S/N. The ratio of thickness to the cell size is typically between 5-10. Even for slightly inclined tracks charge will be shared by many pixels. As a consequence S/N of each pixel could be insufficient for superb time resolution that can be achieved for perpendicular tracks. Trench-3D offer clear advantage over Column-3D, as larger cells offer better time resolution providing that the spatial resolution is adequate.

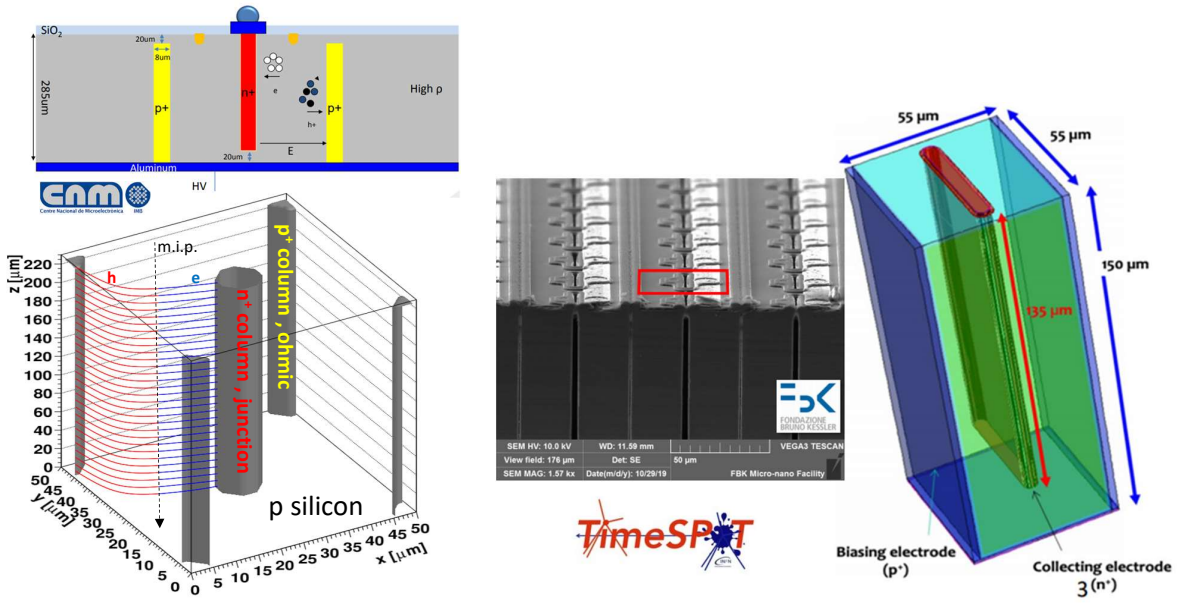

(a) (b)

Figure 7: 3D detectors for 4D tracking applications: (a) Column-3D and (b) Trench-3D.

5. Conclusions and directions for the future

The sensor technologies for 4D tracking will require accompanying electronics. Although developments in electronics are very fast the accessibility to these technologies for particle physics is not straightforward. The required functionalities to be hosted in the pixel are complex. The gains of smaller feature size are not clear for the analog part (28 nm and lower CMOS processes), but are obvious for the required digital functionalities that should be hosted in the small cell: TDC, data processing logic, memory buffer etc. The advantage of hybrid approach over the monolithic one is more flexibility in mixing the technologies.

Fast electronics with large capacitance at the input, either thin LGADs or 3Ds, will require larger power consumption posing a difficulty for cooling. Current ASICs (ALTIROC [2], ETROC [3]) aiming for $\sim$ 30 ps resolution in LGADs with the above functionalities require several hundreds of mW/cm^2 and achieve the jitter of $\sim 20-40\frac{\text{ps fC}}{\text{pF}}C_d/Q_{tresh}$, where C_d is the capacitance of the pad/pixel and Q_{tresh} threshold applied in the ASIC (ToA).

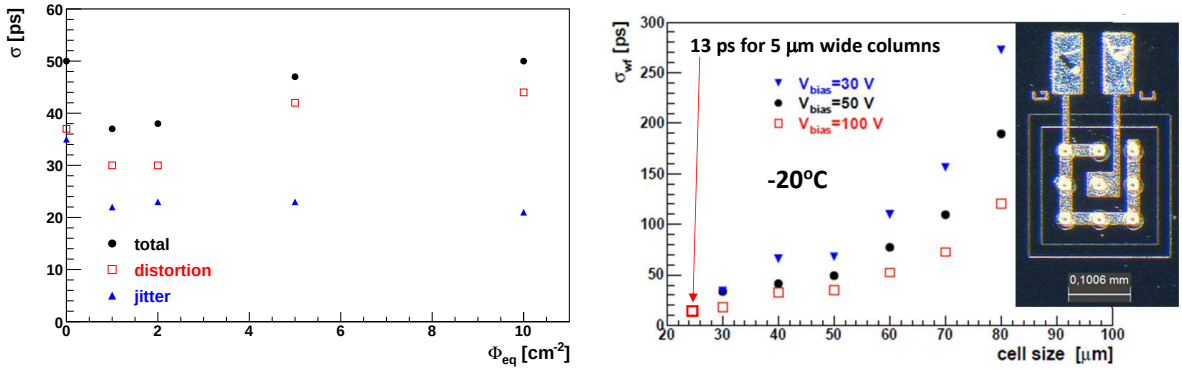

Figure 8: (a) Measured time resolution for a $50 \times 50\,\mu m^2$ single cell device with ^{90}Sr electrons and readout with discrete electronics at $-20°C$. The dominant contributions to time resolutions are shown. (b) Simulated σ_{wf} for perpendicular impact across the cell of the device at different bias voltages for a non-irradiated sensor. Note that apart from the smallest cell simulated columns were 8 μ m wide. The photo shows the measured and simulated device.

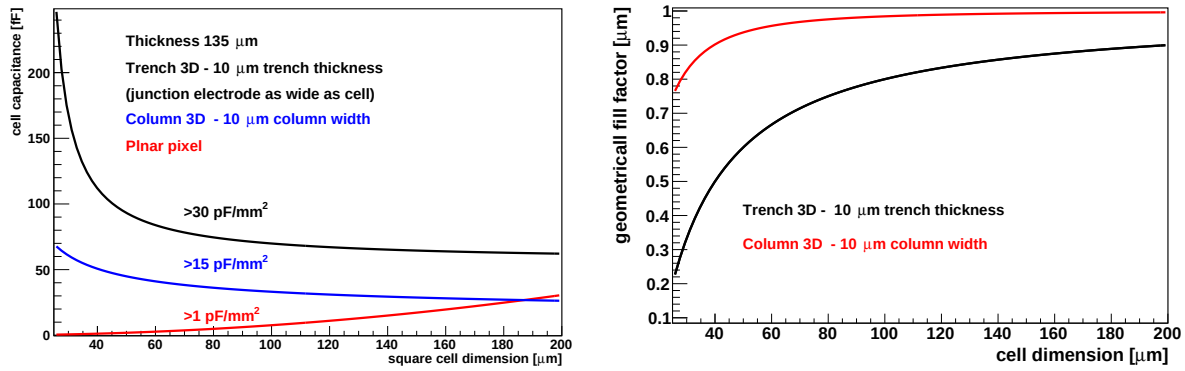

(a) (b)

Figure 9: (a) Dependence of calculated square cell capacitance on cell dimension for a 135 μm thick planar and 3D detectors with columns and trenches extending over the entire thickness. (b) Dependence of geometrical fill factor for perpendicular tracks for the same cells as in (a).

The direction in the future developments will likely go in utilizing internal gain also in CMOS devices and possibly also in 3D detectors. The improvements of aspect ratio (DRIE) could lead to electrodes/trenches of smaller diameter/dimensions and hence reduced capacitance and better fill factor. Column geometry affects electric field focusing in 3D detectors and for narrow columns may lead to controlled impact ionization. A development of monolithic 3D sensors may be also one of the research directions.

References

[1] ATLAS and CMS collaborations, "Report on the Physics at the HL-LHC, and Perspectives for the HE-LHC", CERN-2019-007, 2019.

[2] ATLAS Collaboration, “Technical Design Report: A High-Granularity Timing Detector for the ATLAS Phase-II Upgrade”, CERN-LHCC-2020-007 ; ATLAS-TDR-031.

[3] CMS Collaboration, “A MIP Timing Detector for the CMS Phase-2 Upgrade”, CERN-LHCC-2019-003 (2019).

[4] A. Abada et al.,"FCC-hh: The Hadron Collider", The European Physical Journal Special Topics volume 228 (2019) p. 755–1107.

[5] T. Pajero et al.,"VELO Upgrade II The LHCb 4D pixel detector", this proceedings.

[6] G. Aglieri Rinella et al., "The NA62 GigaTracKer: a low mass high intensity beam 4D tracker with 65 ps time resolution on tracks", JINST 14 (2019) P07010.

[7] M Moulson et al., "KLEVER: An experiment to measure BR($K_L \to \pi^0 \nu\bar{\nu}$) at the CERN SPS", J. Phys.: Conf. Ser. 1526 (2020) 012028.

[8] N. Abgrall et al.,"NA61/SHINE facility at the CERN SPS: beams and detector system", JINST 9 (2014) no. 06, P06005.

[9] A. Abada et al.,"FCC-ee: The Lepton Collider", The European Physical Journal Special Topics volume 228, pages261–623 (2019).

[10] F. U. Pur et al., “Feasibility study of a proton CT system based on 4D-tracking and residual energy determination via time-of-flight”, Phys. Med. Biol. 67 (2022) 095005.

[11] A. Vignati et al., “Innovative thin silicon detectors for monitoring of therapeutic proton beams: preliminary beam tests”, JINST Vol. 12 (2017) C12056

[12] S. Parker et al., "3D - A proposed new architecture for solid-state radiation detectors", Nucl. Instr. and Meth. A 395 (1997) 328.

[13] G. Pellegrini et al., “Technology developments and first measurements of Low Gain Avalanche Detectors (LGAD) for high energy physics applications”, Nucl. Instr. and Meth. A 765 (2014) 12.

[14] H.F-W. Sadrozinski, A. Seiden, N. Cartiglia, “4D tracking with ultra-fast silicon detectors”, REPORTS ON PROGRESS IN PHYSICS 81(2) 026101, 2018.

[15] I. Perić et al., "Particle pixel detectors in high-voltage CMOS technology—New achievements", Nucl. Inst. and Meth. A650 (2011) 158.

[16] W. Snoeys et al., "A process modification for CMOS monolithic active pixel sensors for enhanced depletion, timing performance and radiation tolerance", Nucl. Inst. and Meth. A871 (2017) 60.

[17] S. Meroli et al., "Energy loss measurement for charged particles in very thin silicon layers", JINST 6 (2011) P06013.

[18] kdetsim.org

[19] G. Kramberger et al., “Radiation effects in Low Gain Avalanche Detectors after hadron irradiations”, JINST Vol. 10 (2015) P07006.

[20] M. Ferrero et al,"Radiation resistance LGAD design", Nucl. Inst. and Meth. A919 (2019) 16.

[21] G. Kramberger et al., “Radiation hardness of thin low gain avalanche detectors”, Nucl. Instr. and Meth. A 891 (2018) 68.

[22] G. Lindström et al., “Radiation hard silicon detectors - developments by the RD48 (ROSE) collaboration”, Nucl. Instr. and Meth. A 466 (2001) 308.

[23] G. L. Medin et al.,"Femtosecond laser studies of the Single Event Effects in Low Gain Avalanche Detectors and PINs at ELI Beamlines", Nucl. Instr. and Meth. A 1041 (2022) 167321.

[24] R. Heller et al.,"Systematic study of heavily irradiated LGAD stability using the Fermilab Test Beam Facility", presented at 40^{th} RD50 workshop, CERN, (2022).

[25] V. Sola et al."A compensated design of the LGAD gain layer", Nucl. Instr. and Meth. A 1040 (2022) 167232.

[26] K. Hara et al., "Improvement of timing resolution and radiation tolerance for finely segmented AC-LGAD sensors", presented at TREDI Workshop, Trento, Italy (2023).

[27] G. Kramberger et al., "High temperature annealing of irradiated LGADs", presented at 40^{th} RD50 workshop, CERN, (2022).

[28] E. Curras et al., "Inverse Low Gain Avalanche Detectors (iLGADs) for precise tracking and timing applications", Nucl. Instr. and Meth. A 958 (2000) 162545.

[29] M. Mandurrino, "Demonstration of 200-, 100-, and 50- μm pitch resistive AC-coupled silicon detectors (RSD) with 100% fill-factor for 4D particle tracking", IEEE Electron Device Lett., 40 (11) (2019) 1780.

[30] L. Menzio et al., "DC-coupled resistive silicon detectors for 4D tracking", Nucl. Instr. and Meth. A 1041 (2022) 167374.

[31] G. Paternoster et al., "Trench-Isolated Low Gain Avalanche Diodes (TI-LGADs)", IEEE Electron Device Lett., 41 (6) (2019), p. 884,

[32] M. Senger et al., "Characterization of timing and spacial resolution of novel TI-LGAD structures before and after irradiation", Nucl. Instr. and Meth. A 1039 (2022) 167030.

[33] L. Paolozzi et al.,"Picosecond Avalanche Detector — working principle and gain measurement with a proof-of concept prototype", JINST 17 (2022) P10032.

[34] S. Parker et al., “Increased Speed: 3D Silicon Sensors; Fast Current Amplifiers”, IEEE Trans. Nucl. Sci. 58(2) (2011), p. 404.

[35] G. Kramberger et al., "Timing performance of small cell 3D silicon detectors", Nucl. Instr. and Meth. A 934 (2019) 26.

[36] C. Betancourt et al., "Time Resolution of an Irradiated 3D Silicon Pixel Detectors", Instruments 6 (2022) 12.

[37] R. Mendicino et al., "3D Trenched-Electrode Sensors for Charged Particle Tracking and Timing", Nucl. Instr. and Meth. A927 (2019) 24.

[38] L. Anderlini et al., "Intrinsic time resolution of 3D-trench silicon pixels for charged particle detection", JINST 15 (2020) P09029.

[39] J. Lange et al., "Radiation hardness of small-pitch 3D pixel sensors up to a fluence of 3×10^{16} n_{eq}/cm^2", JINST vol. 13 (2018) P09009.